BASIC SCIENCES

Aortic Gene Expression Profiles Show How ApoA-I Levels Modulate Inflammation, Lysosomal Activity, and Sphingolipid Metabolism in Murine Atherosclerosis

Marco Busnelli [iD],* Stefano Manzini [iD],* Matteo Chiara, Alice Colombo [iD], Fabrizio Fontana, Roberto Oleari, Francesco Potì [iD], David Horner, Stefano Bellosta [iD], Giulia Chiesa [iD]

OBJECTIVE: HDL (high-density lipoprotein) particles are known to possess several antiatherogenic properties that include the removal of excess cholesterol from peripheral tissues, the maintenance of endothelial integrity, antioxidant, and anti-inflammatory activities. ApoA-I overexpression in apoE-deficient (EKO) mice has been shown to increase HDL levels and to strongly reduce atherosclerosis development. The aim of the study was to investigate gene expression patterns associated with atherosclerosis development in the aorta of EKO mice and how HDL plasma levels relate to gene expression patterns at different stages of atherosclerosis development and with different dietary treatments.

APPROACH AND RESULTS: Eight-week-old EKO mice, EKO mice overexpressing human apoA-I, and wild-type mice as controls were fed either normal laboratory or Western diet for 6 or 22 weeks. Cholesterol distribution among lipoproteins was evaluated, and atherosclerosis of the aorta was quantified. High-throughput sequencing technologies were used to analyze the transcriptome of the aorta of the 3 genotypes in each experimental condition. In addition to the well-known activation of inflammation and immune response, the impairment of sphingolipid metabolism, phagosome-lysosome system, and osteoclast differentiation emerged as relevant players in atherosclerosis development. The reduced atherosclerotic burden in the aorta of EKO mice expressing high levels of apoA-I was accompanied by a reduced activation of immune system markers, as well as reduced perturbation of lysosomal activity and a better regulation of the sphingolipid synthesis pathway.

CONCLUSIONS: ApoA-I modulates atherosclerosis development in the aorta of EKO mice affecting the expression of pathways additional to those associated with inflammation and immune response.

GRAPHIC ABSTRACT: A graphic abstract is available for this article.

Key Words: aorta ■ atherosclerosis ■ inflammation ■ osteoclast ■ transcriptome

C ardiovascular disease, once the main cause of death in the Western world, now outranks all other death risk factors on a global scale, according to the World Health Organization.[1]

Atherosclerosis, the underlying pathology of several cardiovascular diseases, elicits a chronic inflammation of the vascular wall and can initiate as early as in childhood. These early vascular structural alterations develop over time and are typically diagnosed only at a late stage.[2]

High blood cholesterol levels—especially if carried by apoB$_{100}$-containing lipoproteins—promote atherosclerotic cardiovascular disease. Circulating LDL (low-density

Arterioscler Thromb Vasc Biol is available at www.ahajournals.org/journal/atvb

Nonstandard Abbreviations and Acronyms	
DE	differentially expressed
EKO	apolipoprotein E knockout
EKO/hA-I	EKO mouse, transgenic for human apoA-I
HDL	high-density lipoproteins
HDL-C	high-density lipoproteins cholesterol
LDL	low-density lipoproteins
LDLrKO	LDL receptor knockout
NLD	normal laboratory diet
TF	transcription factor
VLDL	very-low-density lipoprotein
WD	Western-type diet
WT	wild type

Highlights

- First ever detailed high-throughput RNA-seq analysis of the aorta of apolipoprotein E knockout (EKO) mice overexpressing human apoA-I (EKO/hA-I).
- EKO/hA-I mice have plasma total cholesterol levels comparable to EKO mice, but express apoA-I at thrice EKO levels, display a restored HDL (high-density lipoprotein) peak, and develop far less atherosclerosis than EKO.
- Atherosclerosis reduction in EKO/hA-I, besides a reduced inflammation, is dependent on reduced lysosomal, phagosomal, and osteoclast differentiation pathways, similar to wild type.
- EKO/hA-I show reduced sphingolipid metabolism, that in turn may further reduce the inflammation and atherosclerosis development.

lipoprotein) particles can accumulate in the intima, the innermost layer of the artery, through ionic interactions with proteoglycans of the extracellular matrix.[2,3] Trapped particles are prone to oxidative modifications that initiate (as fatty streaks) and promote the development of the vascular lesions into more mature plaques.[4]

On the contrary, elevated HDL (high-density lipoprotein) levels are considered to be antiatherogenic, despite the fact that therapies aimed at increasing HDL-C (HDL-cholesterol) levels have not still yielded the foreseen clinical benefits.[5] Recently, it has been suggested that the inverse correlation between cardiovascular disease risk and HDL levels is more complex than previously believed, being U-shaped rather than linear.[6,7] Furthermore, recent evidence suggests that rather than with absolute HDL-C levels, the effective cholesterol efflux capacity from macrophages to nascent HDL particles—consistently highlighted by studies on animal models[8–11]—correlates with a reduced cardiovascular risk in humans.[12,13] HDL has been shown to slow the development of atherosclerosis by protecting the endothelium, inhibiting LDL oxidation, playing an important role in host defence, and exerting anti-inflammatory and antithrombotic effects.[14–16]

As in humans, hypercholesterolemia also triggers the development of atherosclerosis in mice. Hypercholesterolemia in mice develops by targeted knockout of cholesterol metabolism related genes, the most common being the LDLrKO (LDL receptor) and the apoEKO (EKO).[17] EKO mice are by far the most exploited mouse model for the study of atherosclerosis, as they readily develop lesions, resembling human ones, even without any dietary challenge, unlike LDLrKO. They have been successfully employed to study the onset and development of atherosclerosis, as well as in proof of concept studies aimed at the prevention of the disease, including drug discovery.[18,19]

ApoE plays a major role in the clearance of non-HDL lipoproteins, thus its deletion causes severe hypercholesterolemia.[20] Additionally, as apoE is also a protein component of HDL particles, its ablation severely reduces HDL concentration,[21,22] which can be restored to physiological levels through the overexpression of human apoA-I.

To elucidate how different dyslipidemic conditions can impact on gene expression levels, and to identify gene expression patterns specifically associated with either genotype, age, and dietary treatment conditions, we employed RNA-seq to analyze the transcriptome of 3 mouse models: atherosclerosis-prone EKO and EKO mice overexpressing human apoA-I (EKO/hA-I), plus their common background, the C57BL/6J as a control (wild type [WT]). In addition to the genotype, the main driver of atherosclerosis development, we further refined our characterization by including 2 dietary treatments (normal laboratory diet [NLD] and Western-type diet [WD], nonatherogenic and atherogenic, respectively) and 2 time points (early and late stage of atherosclerosis development).

Herein, we present a comprehensive picture of the transcriptional profiles of these models, along with a detailed description of the modulated pathways related to specific experimental conditions. We found that genotype accounts for most of the transcriptional changes, and all comparisons involving this experimental set display enrichment of gene ontology terms/KEGG (Kyoto encyclopedia of genes and genomes) pathways mainly related to lipid metabolism/signaling and immune response, particularly to phagosome-lysosome activity.

MATERIALS AND METHODS

All data and materials have been made publicly available at NCBI GEO (Gene Expression Omnibus) Data sets and can be accessed at (https://www.ncbi.nlm.nih.gov/geo/query/acc.cgi?acc=GSE163657).

Animals and Experimental Procedures

Procedures involving animals and their care were conducted in accordance with institutional guidelines that are in compliance with national (D.L. No. 26, March 4, 2014, G.U. No. 61, March 14, 2014) and international laws and policies (EEC Council Directive 2010/63, September 22, 2010: Guide for the Care and Use of Laboratory Animals, United States National Research Council, 2011). The experimental protocol was approved by the Italian Ministry of Health (Protocollo 2012/4).

WT C57BL/6J and EKO mice (https://www.jax.org/strain/002052) in the C57BL/6J background were purchased from Charles River Laboratories (Calco, Italy); Apoa1 knockout mice, also in the C57BL/6J background, were kindly provided by Dr N. Maeda[23]; EKO/hA-I were obtained by multiple crosses between EKO mice and hemizygous mice overexpressing human apoA-I[24,25]; polymerase chain reaction primers used for screening are listed in Table I in the Data Supplement. To prevent the possible impact of hormonal changes of female mice on the results, only male mice were enrolled in the study.

Eight-week-old male mice were randomly divided into 4 groups of 8 mice and fed a NLD (4RF21, Mucedola, Italy) or a Western diet (WD, TD.88137, Envigo, Italy) for 6 or 22 weeks. One week before the end of the dietary treatment, after an overnight fast, mice were anesthetized with 2% isoflurane (Merial Animal Health, Woking, United Kingdom). Blood was collected from the retro-orbital plexus into tubes containing 0.1% (w/v) EDTA and centrifuged in a microcentrifuge for 10 minutes at 5900g at 4 °C.

At the end of the dietary treatments, mice were euthanized under general anesthesia with 2% isoflurane (Merial Animal Health, Woking, United Kingdom), and blood was removed by perfusion with 1× PBS. The aorta was rapidly dissected from the aortic root to the iliac bifurcation, and periadventitial fat was removed. Aortas were then snap-frozen in liquid nitrogen for RNA-seq analyses (n=3) or longitudinally opened, pinned flat on a black wax surface in ice-cold PBS, and photographed unstained for en face analysis (n=3–9).[26–29] For the histological evaluation of the aortic sinus, hearts were harvested, processed, and stained with haematoxylin and eosin as previously described (n=3–6).[26–29] Both aortic en face and aortic sinus histology were performed in accordance with American Heart Association recommendations.[30]

Plasma Measurements

Plasma total cholesterol and triglycerides were measured with enzymatic methods (ABX Diagnostics, Montpellier, France; COD: CPA11 A01634 and CPA11 A01640, respectively), and lipid distribution among lipoproteins was analyzed by fast protein liquid chromatography as described.[24]

Plasma human apoA-I concentration was determined by immunoturbidimetric assays, using an antiserum specific for human apoA-I (LTA, Milan, Italy), as previously described.[31] Coomassie staining was used to quantify plasma murine apoA-I and to confirm the immunoturbidimetric quantification of human apoA-I.[32] Purified apoA-I was used as calibration standard.

RNA Extraction

Total RNA was isolated from mouse tissues and extracted as previously described.[33] RNA was quantified and purity was checked, and 1 µg RNA was retrotranscribed to cDNA, as described.[34] Possible gDNA contamination was ruled out by running a polymerase chain reaction on 20 ng of cDNA/RNA with a primer pair producing 2 amplicons of different size on cDNA (193 bp) and gDNA (677 bp), see Srp14, Table II in the Data Supplement.

Quantitative Polymerase Chain Reaction

Twenty nanograms of cDNA were used as template for each quantitative polymerase chain reaction, performed on a CFX Connect thermal cycler with iTAQ Universal Sybr Green Supermix (Bio-Rad, Segrate, Italy). Conditions and primers are detailed in Table II in the Data Supplement. A final melting curve analysis was always performed. Fold changes relative to the control group were calculated with the ΔΔCt method.[35] The gene cyclophilin A (Ppia) was used as reference gene.

RNA-Seq Analyses

The quality of the mRNA was tested using the Agilent 2100 Bioanalyzer (Agilent Technologies, Santa Clara, CA) before RNA-seq; samples with RNA integrity number <7.0 were discarded. RNA samples were processed using the RNA-Seq Sample Prep kit from Illumina (Illumina, Inc, CA). Eight to 9 tagged libraries were loaded on one lane of an Illumina flowcell, and clusters were created using the Illumina Cluster Station (Illumina, Inc, CA). Clusters were sequenced on a Genome Analyzer IIx (Illumina, Inc, CA) to produce 50 nt-long, unpaired reads.

Data Processing and Visualization

Reads were mapped on the Gencode M21 annotation of the *Mus musculus* transcriptome using the bowtie2 program.[36] Estimation of gene expression levels was performed using RSEM.[37] Differential expression analysis was performed applying the quasi-likelihood F test of the edgeR[38] R[39] package to RSEM estimated reads counts. Only genes with >10 reads in at least 4 different biological replicates were considered. Genes showing a false discovery rate <0.05 were considered differentially expressed (DE).

Gene ontology analyses were performed with STRING,[40] and terms with adjusted $P<0.05$ were considered significant. GEO data sets[41] were analyzed with the Geo2R online tool with default parameters; terms with adjusted $P<0.05$ were considered significant.

Pscan[42] was used to identify over-represented TF (transcription factor)-binding-sites using the JASPAR database[43] as matrices.

Hierarchical clustering was performed by Euclidean metric on standard scaled rows.[44] Principal Component Analysis was performed with Scikit-learn.[45]

Data visualization was performed with SciPy,[44] matplotlib,[46] seaborn,[47] and ternary[48] libraries for the Python programming language. Detailed information can be found in the Data Supplement.

Cell Culture and Lysosomal Activity Measurement

Seventy-two hours after IP injection of 4 mL of 4% thioglycollate broth (Brewer thioglycollate medium, Fluka, Sigma
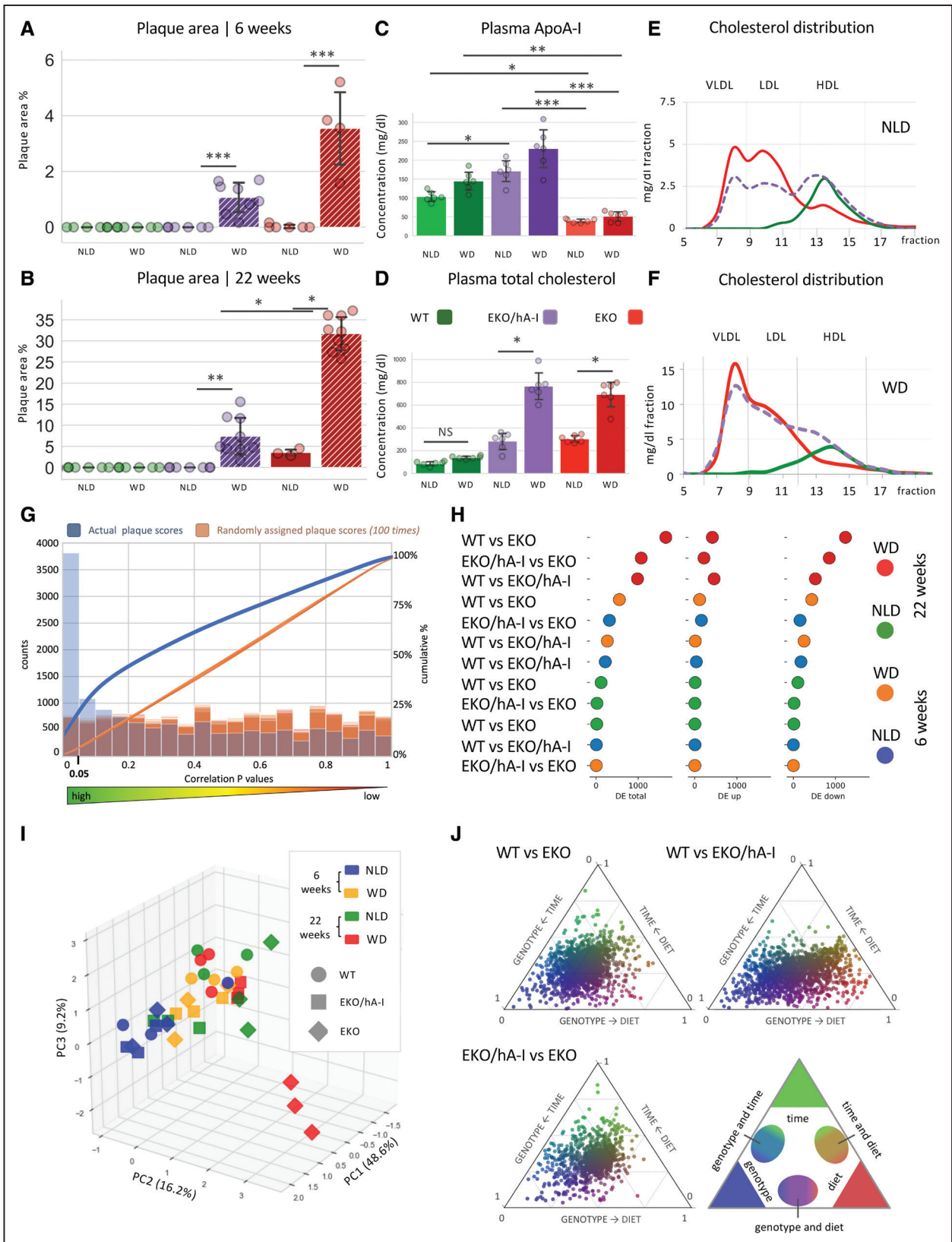
BASIC SCIENCES - AL

Figure 1. Histological/biochemical parameters and data set overview.
Plaque area (percentage, plaque area/total area) was measured in the whole aorta, at 6 wk (**A**) and 22 wk (**B**). In **C**, plasma apoA-I levels measured at 22 wk of normal laboratory diet (NLD) were comparable between wild type (WT) and apolipoprotein E knockout (EKO) mouse, transgenic for human apoA-I (EKO/hA-I), but lower in EKO vs WT (*P*=0.035) and EKO/hA-I (*P*=0.001). ApoA-I levels were slightly increased by Western-type diet (WD), with similar differences (lower in EKO vs WT, *P*=0.007 and vs EKO/hA-I, *P*<0.0001). Total cholesterol levels (n=6, each sample was assayed in duplicate), quantified after 5 h fasting, are shown in **D**. WD resulted in increased total cholesterol (*Continued*)

Aldrich, St. Louis, MO), macrophages were harvested from the peritoneum of euthanized EKO mice with ice-cold PBS, centrifuged, and suspended in DMEM (Dulbecco's modified Eagle's medium) medium (Lonza, Basel, Switzerland) supplemented with penicillin/streptomycin (100 U/mL each; Gibco, Rodano, Milan, Italy) and plated. After one hour, plates were washed, and adherent cells were left for 16 hours in DMEM containing 10% fetal calf serum, then treated with DMEM containing 0.2% BSA (Sigma Aldrich, St. Louis, MO) and either Bafilomycin 1×, acetylated LDL 50 µg/mL (ThermoFisher, Milan, Italy; Catalog No. L35354), or acetylated LDL 50 µg/mL supplemented with increasing concentrations of HDL (100, 250, and 500 µg/mL; Merck, Darmstadt, Germany; Catalog No. LP3-5MG), for 48 hours. Lysosomal activity was measured with a self-quenched substrate, with Bafilomycin 1× as control, following manufacturer's instructions (Lysosomal Intracellular Activity Assay kit, Abcam, Cambridge, United Kingdom; Catalog No. ab234622). Cells were fixed and counterstained with DAPI, then the signal was quantified for each treatment by fluorescence microscopy in 6 randomly chosen 63× fields among biological replicates from 3 independent experiments per group with ImageJ.[49]

Statistical Analyses

Statistical analyses are detailed for each individual analysis in the appropriate figure or table caption. Analyses were performed with R,[39] with packages reshape[50] and dunn.test[51] for Kruskal-Wallis[52] and Dunn[53] post hoc.

RESULTS

Evaluation of Atherosclerosis Development in the Whole Aorta

After 6 weeks on NLD, no atherosclerotic plaques were visible in any genotype, whereas on WD both EKO and EKO/hA-I showed initial, but manifest atherosclerosis, particularly in EKO mice (Figure 1A, Table III and Figure I in the Data Supplement). Twenty-two weeks on NLD resulted in the development of appreciable plaques only in EKO mice. These plaques were comparable in size with those measured after 6 weeks on WD. As expected, 22 weeks of WD dramatically accelerated lesion development in EKO mice and increased atherosclerosis in EKO/hA-I, although to a much lesser extent (Figure 1B, Table IV and Figure I in the Data Supplement).

Representative aorta images are shown in Figure 2, clearly indicating that, in both EKO and EKO/hA-I mice, atherosclerosis started developing at the aortic arch and it spread in the thoracic and abdominal segments only at the latest time point and with the dietary challenge (WD).

The histological evaluation of the aortic sinus confirmed that no lesions were detectable in any genotype after 6 weeks at NLD. Only a limited plaque development became evident in EKO/hA-I mice after 6 weeks at WD or 22 weeks at NLD, whereas ≈5× larger plaques were visible in EKO mice. Although plaque development was increased in EKO/hA-I mice after 22 weeks at WD, it was still half of that observed in EKO mice (Figure 3).

ApoA-I and HDL-C Levels Are Significantly Lower in EKO Mice

Reportedly, the ablation of apoE results in lower apoA-I protein plasma levels.[21] Indeed, EKO mice had much lower levels of circulating apoA-I with respect to WT (Figure 1C). The overexpression of the human *APOA1* transgene fully restored apoA-I plasma levels in EKO/hA-I. WD increased apoA-I levels in each genotype (Figure 1C).

Total plasma cholesterol was affected by the dietary treatment (Figure 1D), with WD resulting into greatly increased total cholesterol levels in EKO and EKO/hA-I mice.

In EKO mice on NLD, fast protein liquid chromatography analysis showed a dramatic cholesterol accumulation in the VLDL (very-low-density lipoprotein) and LDL fractions and a greatly reduced HDL-C peak compared with WT mice (Figure 1E). ApoA-I overexpression in the apoE-knockout background (EKO/hA-I mice), restored HDL levels to those of WT, maintaining the strong cholesterol accumulation in the VLDL and LDL fractions, although to a lower extent than in EKO mice. The WD caused a relevant increase of cholesterol in the VLDL and LDL fractions in both EKO and EKO/hA-I mice (Figure 1F). The HDL-C peak in EKO/hA-I mice was again comparable to that of WT mice.

Genotype, Diet, and Time Differently Impact on Aortic Gene Expression

A total of 14 174 transcripts (of the 25 760 according to Gencode annotation of mmu10) were associated with 10

Figure 1 Continued. (TC) levels in EKO/hA-I (*P*=0.015) and EKO (*P*=0.035), while the increase in WT was not significant (*P*=0.15). On NLD, both EKO/hA-I (*P*=0.008) and EKO (0.006) had higher TC levels than WT. Similarly, on WD, both EKO/hA-I (*P*=0.002) and EKO (0.005) had higher TC levels than WT. On both NLD and WD, EKO/hA-I, and EKO showed comparable TC levels. Statistically significant differences (**A**, **B**, **C**, and **D**) were determined with Kruskal-Wallis followed by Dunn post hoc test. Histograms show the average±SD. *P<0.05; **P<0.01; ***P<0.001. TC distribution among plasma lipoproteins by fast protein liquid chromatography is shown on NLD (**E**) and WD (**F**), both at 22 wk. Each profile was obtained from pooled plasma (n=6). To give an overall overview of the correlation between plaque development and changes in gene expression, a Spearman correlation between expression across all samples and plaque burden (given as severity score) was calculated for all genes, and the distribution of the *P* values is shown in **G**. Lines represent cumulative frequencies. Light blue: scores based on actual plaque burden. Orange: scores randomly assigned to samples. Random assignments were done 100× per gene per samples. In **H**, the number of differentially expressed genes (genotype vs genotype comparisons) is shown. The expression level for all genes in each sample has been reduced to 3 principal components (PC), charted in **I**. In **J**, a score has been given to each gene with respect to each variable (genotype, diet, and time). These coordinates are charted in a triplot for each genotype comparison. HDL indicates high-density lipoprotein; LDL, low-density lipoprotein; and VLDL, very-low-density lipoprotein.
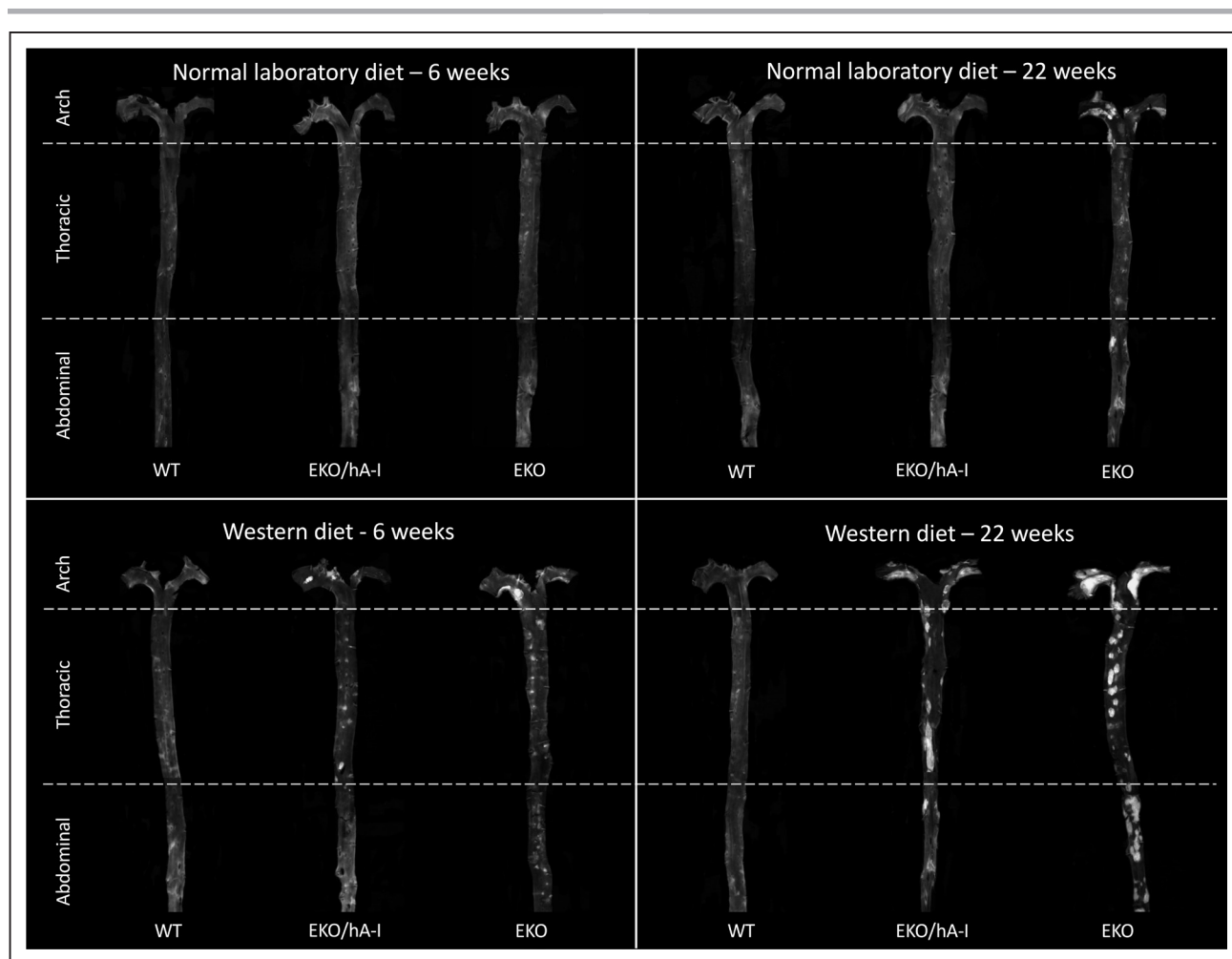
Figure 2. Representative images of aortas prepared with the en face method.
The aorta (n=3 wild type [WT]; n=9 other genotypes) was cut lengthwise and pinned flat onto a black wax surface, and then the exposed plaques (white areas) were quantified as a percentage of the whole aortic area (gray surface). EKO/hA-I indicates EKO mouse, transgenic for human apoA-I.

or more reads in at least 4 independent biological replicate and subjected to differential expression analysis.

The overall expression was comparable among samples (Figure IIA and IIB in the Data Supplement). Transcript abundance estimation was validated by quantitative polymerase chain reaction on 12 genes varying widely in their expression levels and was found to closely match RNA-seq results (Figure III in the Data Supplement).

To evaluate if the expression levels of individual genes would relate to atherosclerosis, lesion severity was graded into 4 tiers: severe (EKO WD 22 weeks), moderate (EKO/hA-I WD 22 weeks), low (EKO NLD 22 weeks, EKO and EKO/hA-I WD 6 weeks), and absent (the remainder of groups). Then—for each gene—the average expression level was tested for correlation (Spearman rank order correlation) with this index. Three thousand eight hundred ten genes showed a good correlation (ρ values ranging from ≈0.9 to ≈0.6) with $P<0.05$, a ≈5-fold increase above the expected value (708 such correlations were expected due to random chance; Figure 1G). This was confirmed by randomly assigning experimental groups into atherosclerosis severity tiers, which failed to reproduce the result (Figure 1G).

Differences in gene expression were compared between genotypes, with matching time and diet (Figure 1H). On average, the number of DE genes was increased by WD, especially at the latest time point.

Dimensionality reduction was performed on gene expression levels for each sample by PCA (principal component analysis; Figure 1I). The diet and the time point had the major impact in the clustering of samples, with the exception of 22 weeks on WD. Six weeks on WD and 22 weeks on NLD had a similar impact on clustering. The atheroprone condition associated with low HDL levels (EKO) produced dramatic changes at 22 weeks on WD, and these samples clustered away from WT and EKO/hA-I samples in the same experimental condition.

Conversely, the impact of the diet, time, and genotype was calculated for each gene (Figure 1J). Differences in gene expression were mostly driven by genotype, followed by dietary treatment, with a lesser contribution of the time variable.
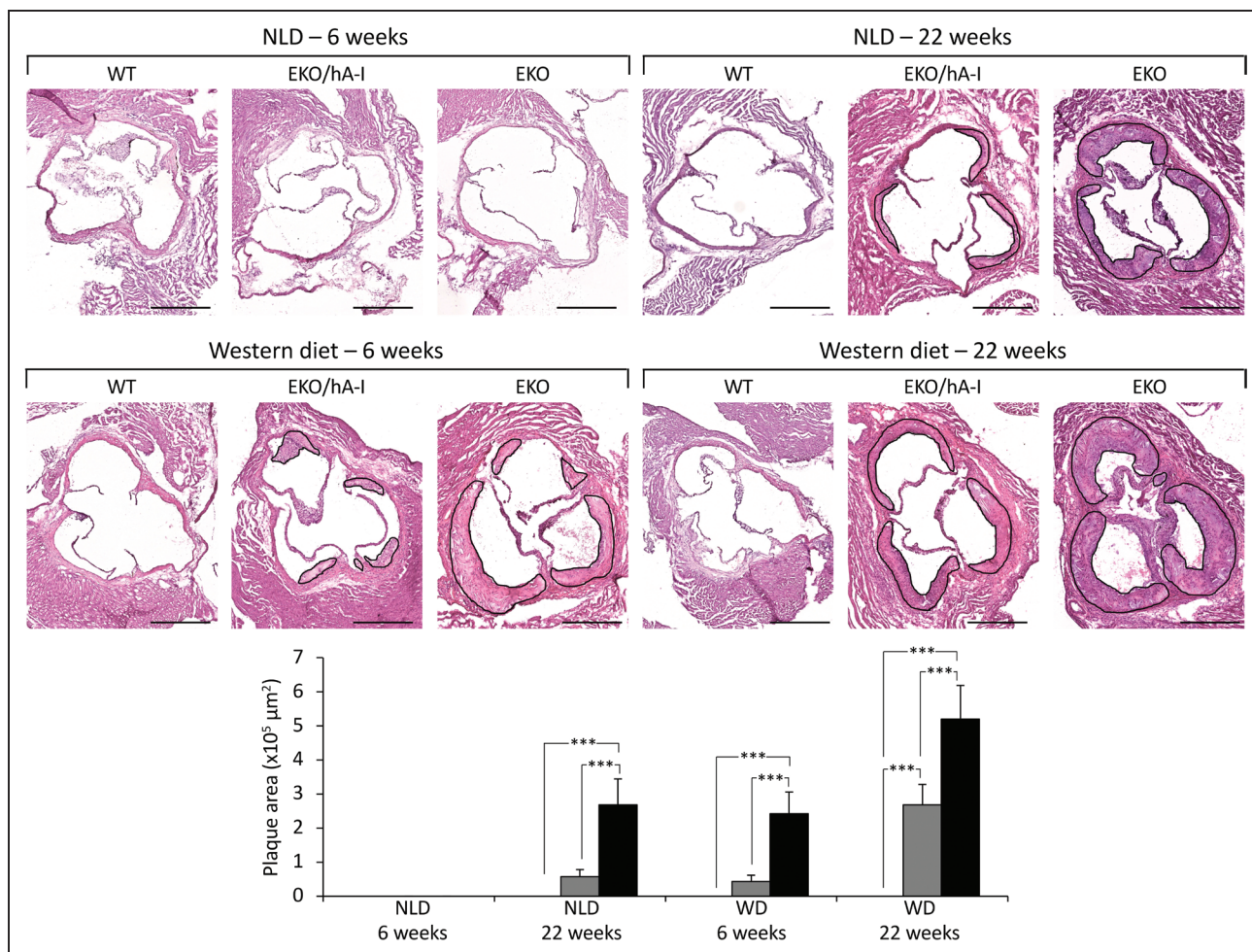
Figure 3. Quantification of atherosclerotic plaque area at the aortic sinus.
Representative haematoxylin and eosin stained pictures of atherosclerosis development at the aortic sinus of wild type (WT), apolipoprotein E knockout (EKO) mouse, transgenic for human apoA-I (EKO/hA-I), and EKO mice (n=3 WT; n=6 other genotypes). Plaques are highlighted with a black continuous line. Data are shown as the mean±SD. NLD indicates normal laboratory diet; and WD, Western-type diet. Bar length=500 µm. ***$P<0.001$.

The comparison between the 2 most different genotypes in terms of plaque development, WT and EKO mice, resulted into the highest number of DE genes (Figure 4A), exacerbated on WD (Figure 4B). The overexpression of the human apoA-I in EKO/hA-I was able to reduce the number of DE genes versus WT, both on NLD and WD (Figure 4C and 4D). On NLD, EKO/hA-I mice were virtually identical to EKO mice, even at 22 weeks despite broad differences in plaque extent (Figure 4E and 4F). After 6 weeks on WD, both genotypes had started developing atherosclerotic lesions, and their transcriptomes were again remarkably similar (Figure 4 L). Conversely, after 22 weeks on WD, when atherosclerosis had rapidly progressed in EKO mice and moderately developed in EKO/hA-I mice, over a thousand DE genes were detected (Figure 4L).

Comparison With Published Data Sets

There are 2 GEO data sets with characteristics similar to our study. Both are microarray-based and feature fewer experimental conditions. The intersection of data from the present work with accession GSE40156,[54–56] analyzing aortas of normal diet-fed WT and EKO mice at 6 and 32 weeks, is remarkable (Figure IVD and IVF in the Data Supplement). Likewise, the intersection with accession GSE31947,[57] analyzing the expression profile in aortas of WD-fed WT and EKO mice is robust (Figure VB in the Data Supplement).

For completeness, the intersection with a more recent work on EKO mice fed either NLD or WD for 6 weeks is shown in Figure VI in the Data Supplement.[58]

Functional Enrichment Analysis Shows That Human ApoA-I Overexpression Strongly Reduces Aortic Inflammation-Related Pathways

A KEGG pathway enrichment analysis of DE genes was performed.

NLD, 6 Weeks

After 6 weeks on NLD, although no aortic plaques were detected in any genotype, an increased
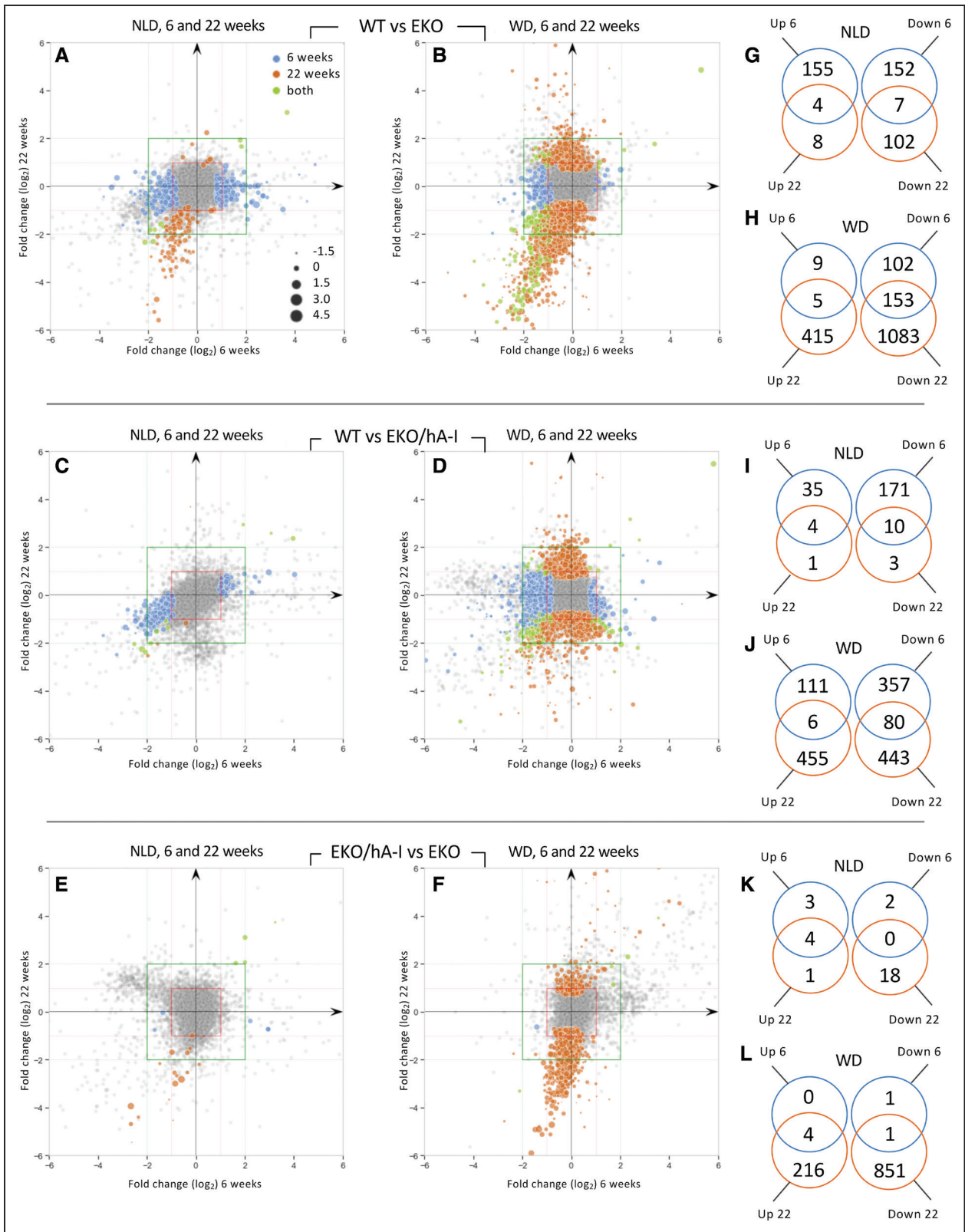
Figure 4. Scatter plots of gene expression levels for all genotype comparisons.
A–F, For each genotype/genotype comparison, the log$_2$ fold change of all genes is charted for 6 wk (*x* axis) and 22 wk (*y* axis), separately for each diet. Genes are marked in blue if differentially expressed (DE) at 6 wk only, in orange if DE at 22 wk only, and in green if DE at both 6 and 22 wk. Genes that follow the same expression pattern over time would align to the x=y line; genes that change their expression pattern would align to the x=−y line. Genes that are not DE are marked in gray. Square boxes help visualizing the 2-fold change (red box, log$_2$FC=1) and 4 fold change (green box, log$_2$FC=2) boundaries. At the right (**G–L**), Venn diagrams summarize the characteristics of each comparison. EKO/hA-I indicates EKO mouse, transgenic for human apoA-I; NLD, normal laboratory diet; WD, Western-type diet; and WT, wild type.

expression of genes involved in the Complement and coagulation cascades (mmu04610) was observed in both EKO and EKO/hA-I versus WT mice (Figure 5). An increased expression of genes involved in the oxidative phosphorylation (mmu00190) was observed in athero-resistant WT mice versus atheroprone EKO mice (Figure 5).

NLD, 22 Weeks

The administration of NLD for 22 weeks led to a slight plaque development only in EKO, and several inflammation-related pathways such as lysosome (mmu04142), phagosome (mmu04145), osteoclast differentiation (mmu04380), and complement/coagulation cascades (mmu04610) were enriched in EKO compared with WT, but not in WT compared with EKO/hA-I (Figure 5). Although the comparison between EKO and EKO/hA-I at this time point did not reveal enriched pathways,

EKO mice had considerably higher expression of genes related to both the innate and adaptive immune system, such as Cdl5, Isg20, Lgals3, and Clec7a, as well as genes required for the extracellular matrix remodeling, such as Mmp12 and Adam8 (Figure 6).

WD, 6 Weeks

After 6 weeks at WD, a generalized activation of the immune system was observed in atheroprone genotypes. Complement/coagulation cascades (mmu04610), osteoclast differentiation (mmu04380), and lysosome (mmu04142) pathways were enriched in both EKO and EKO/hA-I versus WT (Figure 5). No differences were observed when comparing EKO and EKO/hA-I.

WD, 22 Weeks

The most extreme differences were observed in this comparison. Vascular smooth muscle contraction
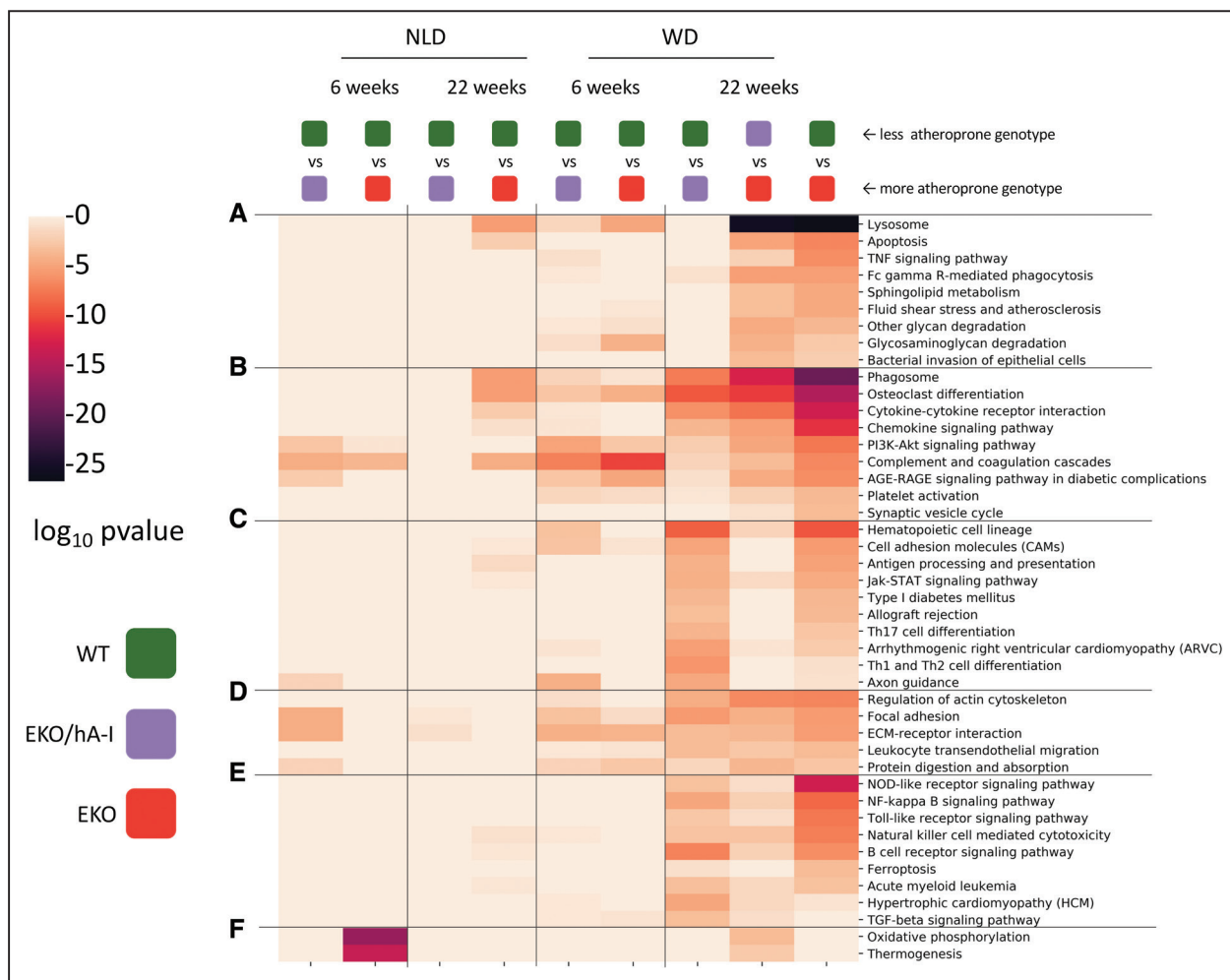
Figure 5. Aggregated results from functional enrichment analysis.
A functional enrichment analysis has been performed for the differentially expressed genes in each genotype/genotype comparison, indicated on **top**. The heatmap shows the P values for each Kyoto encyclopedia of genes and genomes (KEGG) pathway, listed on the **right**. KEGG pathways, selected among enriched pathways with $P<0.0001$, and related to inflammation and metabolism, were clustered into 5 patterns. **A**, Common pathways in wild type (WT) and apolipoprotein E knockout (EKO) mouse, transgenic for human apoA-I (EKO/hA-I) vs EKO; (**B**) growing number of genes from less to more atheroprone; (**C**) common pathways in EKO/hA-I and EKO vs WT; (**D**) similar P values in all 3 genotypes; (**E**) enriched at latest time point on Western-type diet (WD). **F**, higher in WT at 6 wk on normal laboratory diet (NLD). On NLD, 6 and 22 wk, as well as on WD, 6 wk, there were no enriched KEGG pathways in WT vs EKO/hA-I; therefore, the column is not present in the figure.

Figure 6. Details of the differences between apolipoprotein E knockout (EKO) mouse, transgenic for human apoA-I (EKO/hA-I) and EKO on normal laboratory diet (NLD) at 22 wk.
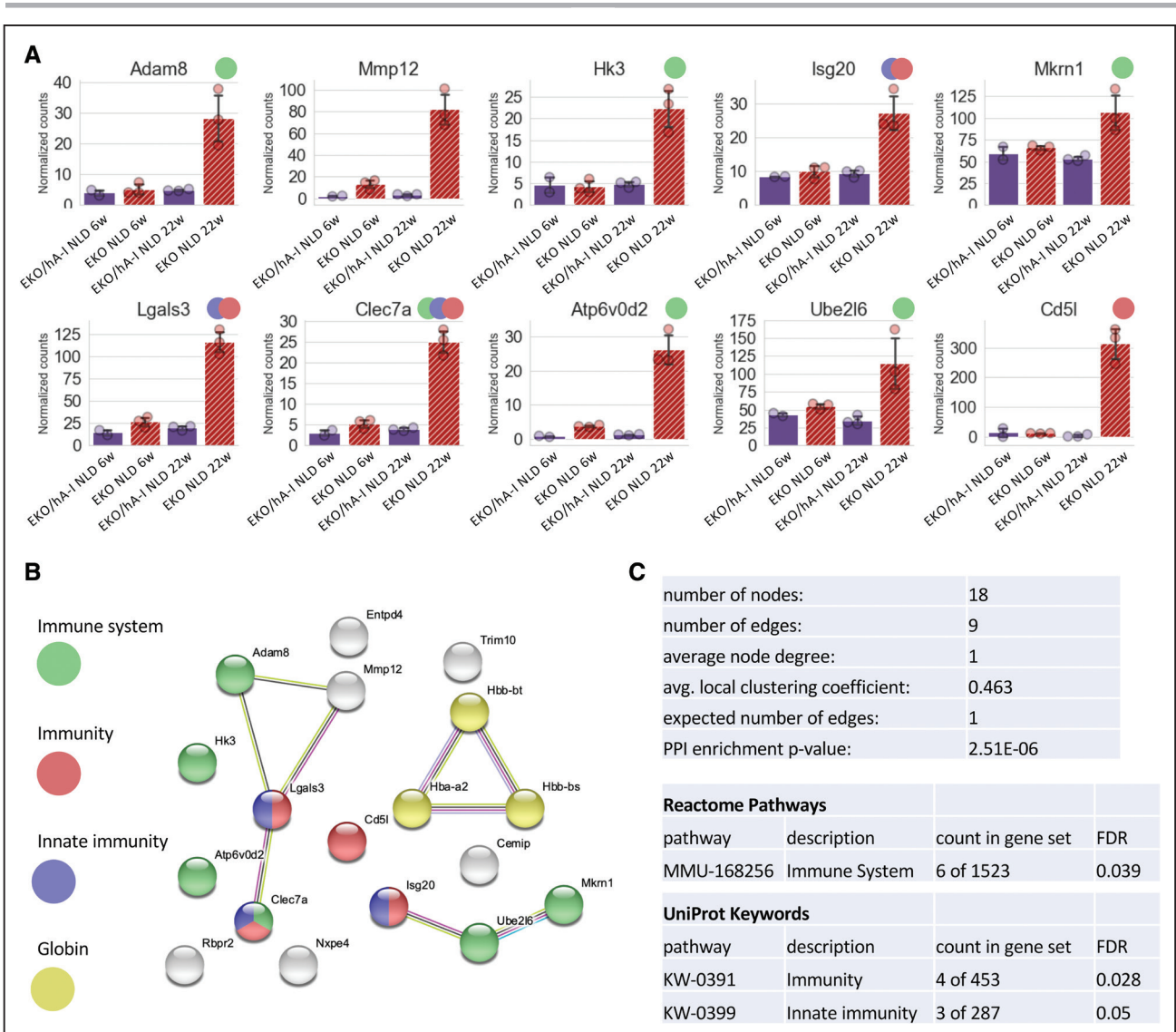Although the differentially expressed genes were not sufficient to result into any enriched pathway, EKO mice had considerably higher expression of genes related to the immune system, charted in **A**. The interaction network of related proteins is shown in **B**. The statistics and details of these interactions are summarized in **C**. FDR indicates false discovery rate; and PPI, protein-protein interaction.

(mmu04270), oxytocin signaling (mmu04921), and focal adhesion (mmu04510) pathways were enriched in WT compared with EKO and EKO/hA-I (Figure VII in the Data Supplement).

The comparison between EKO mice and both WT and EKO/hA-I showed the strongest enrichment in pathways such as lysosome (mmu04142), phagosome (mmu04145), osteoclast differentiation (mmu04380), cytokine-cytokine receptor interaction (mmu04060), Fc gamma R-mediated phagocytosis (mmu04666), apoptosis (mmu04210), TNF signaling (mmu04668), fluid shear stress and atherosclerosis (mmu05418), other glycan degradation (mmu00511), chemokine signaling pathway (mmu04062; Figure 5 and Figure VIII through XVII in the Data Supplement). Overall, the expression of

a large number of genes encoding for cytokines, chemokines, and their receptors closely followed plaque burden (Figure XVIII in the Data Supplement). In addition, genes involved in cholesterol metabolism (mmu04979) and sphingolipid metabolism (mmu00600) were upregulated in EKO (Figure XIX through XXII in the Data Supplement).

Remarkably, the immune system activation was increased in the 2 atheroprone genotypes compared with WT mice (Figure 5), but to a different extent; in fact, although the comparison between WT and EKO/hA-I showed an activation of the immune response in the latter genotype, the direct comparison between EKO and EKO/hA-I clearly showed a reduction in several immune-related pathways in EKO/hA-I mice (Figure XXII in the Data Supplement).

NLD Versus WD, 6 Weeks Versus 22 Weeks

EKO mice showed the strongest enrichment in a large panel of inflammation-related pathways when fed WD in place of the NCD, or when challenged with the HFD for the longer time. On the contrary, only minor changes where appreciable in EKO/hA-I mice in the same comparisons (Figure XXIII in the Data Supplement).

Genes Upregulated in EKO Mainly Relate to Catabolic Processes in Lysosomes

We primarily focused on same-diet, same-time comparisons. We found 2875 genes that were DE at least once, out of 14 174 of the whole data set (Figure 7A). The vast majority was found DE at WD, and at the latest time point (Figure 7B and 7D). A detailed view of the genes that were found DE on 4 or more comparisons is shown in Figure 7C. The overwhelming majority of terms enriched by this set of genes relates to immunity and inflammation (Figure 7E), all intertwined (Figure 7F).

We then focused on the subset of genes that were DE in common between WT and EKO/hA-I when compared with EKO and found 488 of them. In this case also, the vast majority was DE at WD and at 22 weeks (Figure 8A). We found that 453 genes were upregulated in EKO, whereas 35 were downregulated. Their expression level is shown in Figure 8B. The functional enrichment analysis suggests how the genes upregulated in EKO mainly related to catabolic processes regulated by lysosomes and phagosomes (Figure 8C). The genes that were downregulated in EKO conversely related to mitochondrial respiratory chain (Figure 8D). Results for DE genes in diet and time comparisons are summarized in Figure XXIV in the Data Supplement.

DE genes from comparisons containing 20 DE genes or more were scanned in search for motifs of known TFs and 148 were found significantly enriched in 17 different comparisons (Figures XXV and XXVI in the Data Supplement). Interestingly, binding sites for TFEB (transcription factor EB), TFE3 (transcription factor binding to IGHM enhancer 3), and MITF (microphthalmia-associated transcription factor)—TFs involved in lysosomal function and biogenesis[59,60]—were over-represented in EKO mice compared with EKO/hA-I mice.

HDL Reduces Lysosomal Activity In Vitro in LDL-Treated Macrophages

To investigate a possible direct effect of HDL on lysosomal activity, peritoneal macrophages from EKO mice were treated for 48 h with either bafilomycin, which inhibits endocytosis and serves as control (BAF), or acetylated LDL (50 μg/dL), alone or with increasing doses of HDL (100 to 500 μg/dL), these latter conditions mimicking EKO/hA-I. Macrophage exposure to acetylated LDL significantly boosted lysosomal activity, that was progressively reduced by increasing HDL concentrations (Figure XXVII in the Data Supplement).

DISCUSSION

With the aim of identifying new genes/pathways involved in dyslipidemia-driven atherosclerosis, modulated by different apoA-I levels, a transcriptome analysis by high-throughput RNA-seq was conducted on the aorta of 3 mouse models: WT mice, resistant to atherosclerosis development and expressing physiological levels of apoA-I; EKO, with halved apoA-I levels and low HDL-C levels[21]; apoE-knockout mice expressing human apoA-I, with apoA-I and HDL-C levels comparable to those of WT mice (EKO/hA-I).

Mice were fed normal laboratory (low fat, no cholesterol) or WD (high fat, 0.2% cholesterol, total fat 21% w/w), starting from 8 weeks of age, for 6 or 22 weeks.

This comprehensive experimental setup vastly improves on available literature[54–58] of aortic gene expression profiling of WT and EKO mice, by simultaneously comparing different diets and time points. Additionally, gene expression profiling at the aorta of EKO/hA-I mice was never investigated before.

In mice fed NLD, plasma cholesterol levels were comparable between EKO and EKO/hA-I mice and significantly higher than WT mice. The administration of a WD dramatically increased cholesterolemia only in EKO and EKO/hA-I. They are both atheroprone, because of the common EKO background, albeit to a different extent, as manifestly evident in the markedly reduced plaque development in the aorta and at the aortic sinus of EKO/hA-I. This result is in line with previous findings indicating a protective role of human apoA-I overexpression in EKO mice.[21,61]

Diet and genotype were the most impacting variables driving a change in gene expression, with time mostly having a synergistic effect with genotype or with diet rather than per se. The vast majority of genes were significantly DE in genotype comparisons when mice were fed WD and at the latest time point. This effect was likely driven by plaque formation, more pronounced in WD-fed atheroprone genotypes at 22 weeks, and resulting in a number of genes whose expression showed a clear correlation with plaque burden.

The comparison of the WT transcriptome with those obtained from atheroprone mice at the earliest time point on NLD, when plaque development was negligible, indicated an increased mitochondrial activity in WT mice. Reportedly, EKO mice have decreased mitochondrial DNA integrity and mitochondrial respiration, associated with increased reactive oxygen species.[62] The same comparison showed a lower expression of the genes involved in the complement and coagulation cascade in WT mice. Considerable evidence supports the notion that complement and the coagulation cascade act in concert
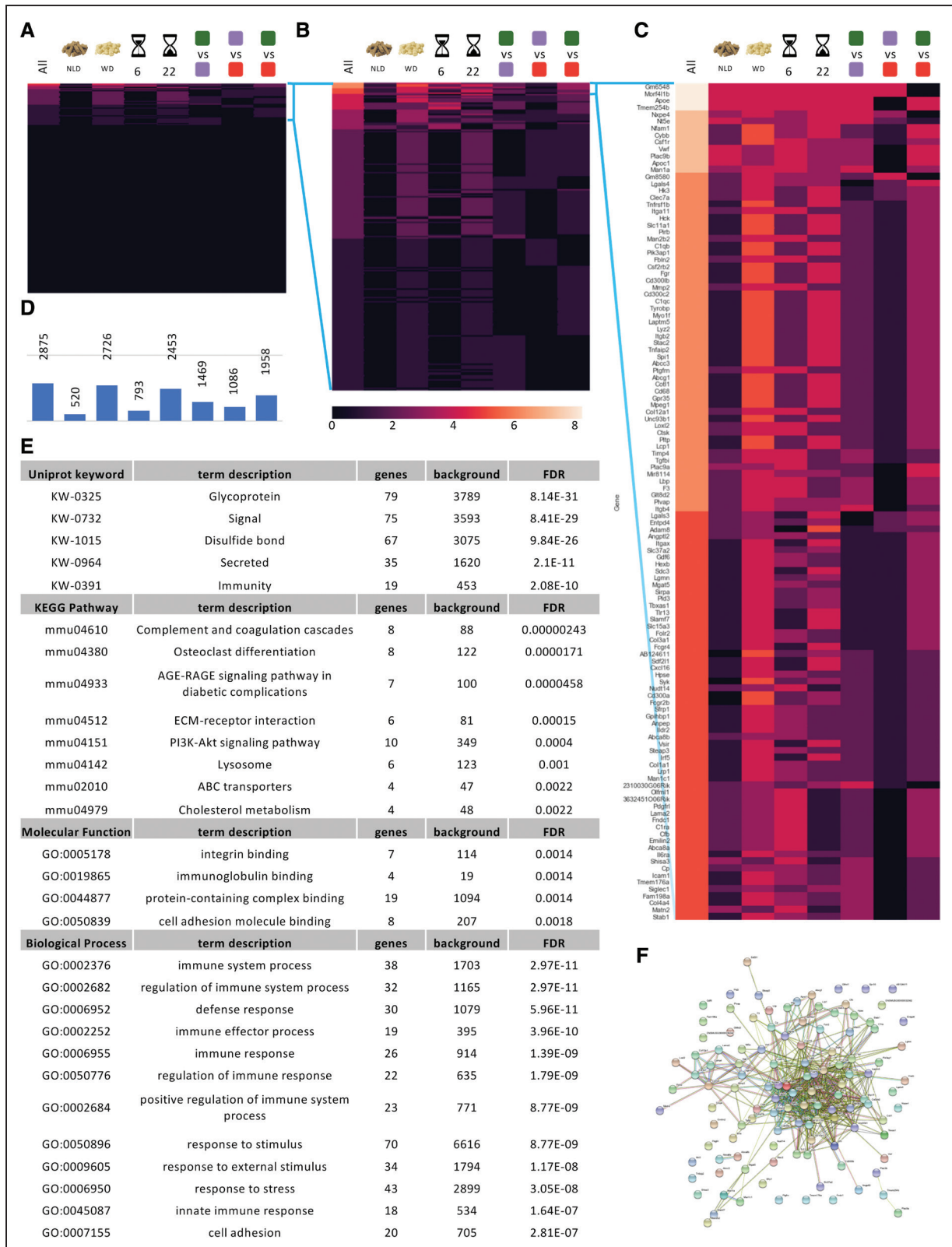
BASIC SCIENCES - AL

E

Uniprot keyword	term description	genes	background	FDR
KW-0325	Glycoprotein	79	3789	8.14E-31
KW-0732	Signal	75	3593	8.41E-29
KW-1015	Disulfide bond	67	3075	9.84E-26
KW-0964	Secreted	35	1620	2.1E-11
KW-0391	Immunity	19	453	2.08E-10
KEGG Pathway	**term description**	**genes**	**background**	**FDR**
mmu04610	Complement and coagulation cascades	8	88	0.00000243
mmu04380	Osteoclast differentiation	8	122	0.0000171
mmu04933	AGE-RAGE signaling pathway in diabetic complications	7	100	0.0000458
mmu04512	ECM-receptor interaction	6	81	0.00015
mmu04151	PI3K-Akt signaling pathway	10	349	0.0004
mmu04142	Lysosome	6	123	0.001
mmu02010	ABC transporters	4	47	0.0022
mmu04979	Cholesterol metabolism	4	48	0.0022
Molecular Function	**term description**	**genes**	**background**	**FDR**
GO:0005178	integrin binding	7	114	0.0014
GO:0019865	immunoglobulin binding	4	19	0.0014
GO:0044877	protein-containing complex binding	19	1094	0.0014
GO:0050839	cell adhesion molecule binding	8	207	0.0018
Biological Process	**term description**	**genes**	**background**	**FDR**
GO:0002376	immune system process	38	1703	2.97E-11
GO:0002682	regulation of immune system process	32	1165	2.97E-11
GO:0006952	defense response	30	1079	5.96E-11
GO:0002252	immune effector process	19	395	3.96E-10
GO:0006955	immune response	26	914	1.39E-09
GO:0050776	regulation of immune response	22	635	1.79E-09
GO:0002684	positive regulation of immune system process	23	771	8.77E-09
GO:0050896	response to stimulus	70	6616	8.77E-09
GO:0009605	response to external stimulus	34	1794	1.17E-08
GO:0006950	response to stress	43	2899	3.05E-08
GO:0045087	innate immune response	18	534	1.64E-07
GO:0007155	cell adhesion	20	705	2.81E-07

Figure 7. Overall comparison, for each variable, of differentially expressed (DE) genes.
The number of times each gene was found differentially expressed in genotype/genotype comparisons is visualized in a heatmap in **A**, with detailed numbers for each column in **D**. The majority of the 14 174 total transcripts were never DE. **B**, Zooming in on the genes that were differentially expressed at least in one comparison. **C**, Details of the genes that were DE in at least 4 comparisons. For these genes, a functional enrichment table is shown in **E**, and their association network is drawn in **F**. AGE-RAGE indicates advanced glycation endproducts-receptor for advanced glycation endproducts; ECM, extracellular matrix; FDR, false discovery rate; GO, gene ontology; KEGG, Kyoto encyclopedia of genes and genomes; and PPI, protein-protein interaction.
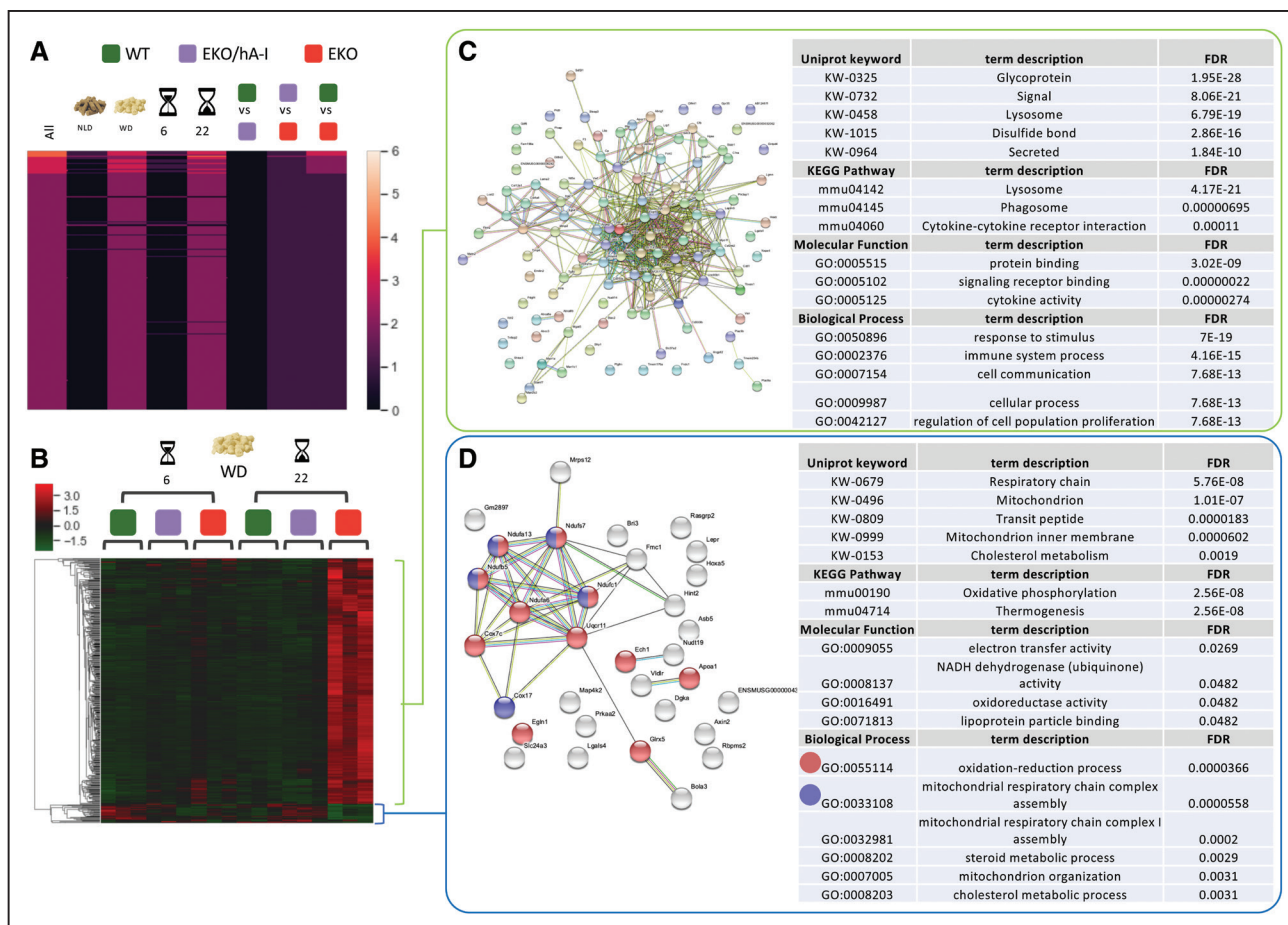
Figure 8. Similarities between wild type (WT) and apolipoprotein E knockout (EKO) mouse, transgenic for human apoA-I (EKO/hA-I) vs EKO.
The number of times each gene was found differentially expressed in WT or EKO/hA-I vs EKO, but not WT vs EKO/hA-I, is visualized in a heatmap (**A**). Expression value Z-scores of these 488 genes are shown in **B**. Changes in gene expression cluster in 2 broad patterns, for which a functional enrichment analysis is detailed for KEGG (Kyoto encyclopedia of genes and genomes pathways) in **C** and **D**. FDR indicates false discovery rate; GO, gene ontology; NLD, normal laboratory diet; and WD, Western-type diet.

to orchestrate the early events that promote plaque formation.[63]

The initial emergence of plaques, such as those observed in EKO and EKO/hA-I mice after 6 weeks on WD or in EKO mice after 22 weeks on NLD, was associated with the activation of the immune system, with several transcripts related to phagocytic activity being upregulated compared with WT.

A huge number of genes indicative of an involvement of both innate and adaptive immunity showed an increased expression when the presence of plaques in the aorta peaked, such as in EKO mice fed WD for 22 weeks compared with WT mice. This result was not unexpected, considering the recognized role played by the immune system in atherosclerosis,[64,65] as well as previous transcriptome profiles obtained from diseased aortic arteries.[66,67]

Additionally, it should be noted that apoE has been recognized to possess anti-inflammatory and immunosuppressive effects and, as a consequence, apoE deficiency in mice is associated with an increased T-cell activation and inflammatory response,[68] accompanied by spleen and lymph node enlargement.[29,69]

In the present study, the most enriched KEGG pathways in EKO, lysosome, phagosome, and osteoclast differentiation were indicative of an increased phagocytic activity.

The activation of the phagocytic-lysosomal pathway in macrophages is considered a critical event in atherosclerotic plaque progression.[70] Lysosomes are small acidic organelles characterized by the activity of up to 60 different hydrolytic enzymes including proteases, lipases, and nucleases. Within macrophages, lysosomes degrade extracellular material, including lipids, via heterophagy, and intracellular material such as lipid droplets, via autophagy.[71] Our results indicate that the heterophagy-mediated lipid uptake was induced in EKO aortas with advanced plaques, being increased the expression of genes encoding for receptor-mediated endocytosis, lysosome membrane proteins, as well as lipases, proteases, glycosidases, sulfatases, one ceramidase and one nuclease, that allow the lysosome to hydrolyse a vast repertoire of biological substrates.

The activation of lysosomal pathways restricted to EKO mice is backed by the finding that, binding sites for TFs involved in lysosome function and biogenesis,[59,60] are over-represented in reads from EKO mice fed WD for 22 weeks with respect to EKO/hA-I. WD treatment results in the same enrichment in EKO, but not in EKO/hA-I mice. Further, acetylated LDL treatment boosted lysosomal activation in EKO-derived peritoneal macrophages, but HDL administration—mimicking the HDL makeup of EKO/hA-I—was able to reduce it in a dose-dependent manner. Conversely, the expression levels of transcripts essential to the formation of the autophagosome, the fundamental organelle for autophagy, were comparable with those found in the healthy aorta of WT mice (Figure XXVIII in the Data Supplement).

Taken together, these results seem to indicate that, in advanced atherosclerosis, autophagosome biosynthesis is unable to match the increased lysosomal activity.

Of note, a reduction of key autophagy markers has been detected in advanced versus early atherosclerotic plaques from mouse and humans.[72] Moreover, the derangement of macrophage autophagy in mice, through genetic ablation of the pivotal autophagy gene Atg5, led to a markedly increased atherosclerosis.[73]

In addition, in the aorta of EKO mice fed WD for 22 weeks, the expression of a large amount of genes involved in osteoclast differentiation was increased. This result is in accordance with previous findings indicating that vascular calcification can take place in advanced atherosclerotic plaques, leading to an excess deposition of calcium phosphate minerals.[74] Vascular smooth muscle cells with an osteoblast-like phenotype promote the differentiation of macrophages to osteoclasts; the secretion of factors driving this differentiation contributes to increasing inflammation and reducing arterial elasticity.[74]

Plaque development was significantly reduced in EKO/hA-I versus EKO mice after 22 weeks on WD. At the transcriptome level, this finding was primarily associated with a strong reduction in the number of genes involved in the immune response. Interestingly, the phagocytic-lysosomal pathway appeared to be less activated in EKO/hA-I compared with EKO mice. Noteworthily, the vast majority of these DE genes annotated in the lysosome, phagosome, and osteoclast differentiation pathways were likewise found, with the same trend, in the comparison between WT and EKO (91%, 81%, and 80%, respectively).

In addition, the expression of genes encoding for several proatherogenic chemokines, such as Ccl2, Ccl3, Ccl4, Ccl6, Ccl7, and Cx3cl1, was reduced in EKO/hA-I mice versus EKO mice. Similarly, a reduced expression of genes coding for receptors such as Ccr5, Cx3cr1, Il13ra1, and Tgfbr1 was observed in EKO/hA-I mice versus EKO mice.

Beyond a dampened activation of the immune system, WT and EKO/hA-I mice also showed a markedly reduced

sphingolipid metabolism, belonging to a complex network of metabolically connected pathways encompassing 40 enzymes. Sphingolipids, mainly ceramide, ceramide-1-phosphate, glucosylceramide, lactosylceramide, sphingosine, sphingosine-1-phosphate, sphingomyelin, and gangliosides are bioactive lipids with a role in cellular regulatory circuits.[75] The results of this study suggest that mice with the largest atherosclerotic plaques have also an increased biosynthesis of ceramide, ceramide-1-phosphate, galactosylceramide, and lactosylceramides (Figure XX in the Data Supplement). The lack of a lipidomic analysis of mouse vessels to support expression data represents a limitation of the present study. However, it should be noted that our observation is in accordance with previous findings indicating that ceramide and lactosylceramide are present in much higher concentrations in human atherosclerotic plaques compared with healthy arteries.[76] We and others have previously demonstrated, in animal models, that increased levels of lactosylceramide and other sphingolipids are associated with the development of atherosclerosis.[27,77,78] Moreover, in humans, the enriched presence of lactosylceramide is associated with an enlarged necrotic core and increased plaque vulnerability.[79]

The accumulation of both ceramide and lactosylceramide may have partially promoted the proinflammatory milieu found in the atherosclerotic vessel: ceramides are able to promote a systemic inflammatory response, whereas lactosylceramide upregulates adhesion molecules on vascular endothelial cells and activates phagocytes, thereby possibly contributing to plaque inflammation.[80,81]

Interestingly, after 22 weeks on WD, a reduced expression of genes with a key role in cholesterol metabolism was observed in EKO/hA-I versus EKO mice, in spite of comparable plasma levels of non-HDL cholesterol. Among them, the genes coding for Lipa (lysosomal acid lipase type A), the transporter Npc1 (Niemann-Pick type C1), Nceh1 (neutral cholesterol ester hydrolase 1), and Abca1 (ATP-binding cassette transporter A1). Notably, the activity of all these genes should prevent foam cell formation and, ultimately, the progression of the atherosclerotic plaque (Figure XI in the Data Supplement). In support of this, it has been demonstrated that their deletion in atheroprone mouse models or the occurrence of loss-of-function mutations in humans worsens atherosclerotic lesion formation.[82–85] Interestingly, the increased expression of these genes, despite a larger plaque area in EKO mice, could be the result of a higher recruitment of monocytes/macrophages in the lesion or it may mean that the response put in place by macrophages is not sufficient to manage the influx of cholesterol.

In conclusion, we present the most comprehensive gene expression profiling of whole aorta of murine atherosclerosis models, by including 2 time points, 2 dietary

treatments, and 3 experimental models with varying degrees of atherosclerosis susceptibility and apoA-I expression. The dissection of the gene expression networks further indicates that an impairment of sphingolipid metabolism, phagosome-lysosome system and osteoclast differentiation, plays a relevant role in atherosclerosis worsening. We confirm the well-known role of inflammation and immune response in atherosclerosis development. Moreover, we add substantial evidence that the reduced atherosclerotic burden in the aorta of EKO mice expressing high levels of apoA-I is accompanied by a reduced activation of the immune system, a reduced involvement of lysosomal activity and a a better regulation of the sphingolipid synthesis pathway.

ARTICLE INFORMATION

Affiliations

Department of Pharmacological and Biomolecular Sciences (M.B., S.M., A.C., F.F., R.O., S.B., G.C.) and Department of Biosciences (M.C., D.H.), Università degli Studi di Milano, Italy. Institute of Biomembranes, Bioenergetics and Molecular Biotechnologies, National Research Council, Bari, Italy (M.C., D.H.). Department of Medicine and Surgery—Unit of Neurosciences, University of Parma, Italy (F.P.).

Acknowledgments

Sources of Funding

Disclosures

None.

REFERENCES

1. Mensah GA, Roth GA, Fuster V. The global burden of cardiovascular diseases and risk factors: 2020 and beyond. *J Am Coll Cardiol.* 2019;74:2529−2532. doi: 10.1016/j.jacc.2019.10.009

2. Libby P, Ridker PM, Hansson GK. Progress and challenges in translating the biology of atherosclerosis. *Nature.* 2011;473:317−325. doi: 10.1038/nature10146

3. Tabas I, Williams KJ, Borén J. Subendothelial lipoprotein retention as the initiating process in atherosclerosis: update and therapeutic implications. *Circulation.* 2007;116:1832−1844. doi: 10.1161/CIRCULATIONAHA. 106.676890

4. Weber C, Noels H. Atherosclerosis: current pathogenesis and therapeutic options. *Nat Med.* 2011;17:1410−1422. doi: 10.1038/nm.2538

5. Tall AR, Rader DJ. Trials and Tribulations of CETP Inhibitors. *Circ Res.* 2018;122:106−112. doi: 10.1161/CIRCRESAHA.117.311978

6. Madsen CM, Varbo A, Nordestgaard BG. Extreme high high-density lipoprotein cholesterol is paradoxically associated with high mortality in men and women: two prospective cohort studies. *Eur Heart J.* 2017;38:2478−2486. doi: 10.1093/eurheartj/ehx163

7. Madsen CM, Varbo A, Tybjærg-Hansen A, Frikke-Schmidt R, Nordestgaard BG. U-shaped relationship of HDL and risk of infectious disease: two prospective population-based cohort studies. *Eur Heart J.* 2018;39:1181−1190. doi: 10.1093/eurheartj/ehx665

8. Out R, Hoekstra M, Habets K, Meurs I, de Waard V, Hildebrand RB, Wang Y, Chimini G, Kuiper J, Van Berkel TJ, et al. Combined deletion of macrophage ABCA1 and ABCG1 leads to massive lipid accumulation in tissue macrophages and distinct atherosclerosis at relatively low plasma cholesterol levels. *Arterioscler Thromb Vasc Biol.* 2008;28:258−264. doi: 10.1161/ATVBAHA.107.156935

9. Out R, Jessup W, Le Goff W, Hoekstra M, Gelissen IC, Zhao Y, Kritharides L, Chimini G, Kuiper J, Chapman MJ, et al. Coexistence of foam cells and hypocholesterolemia in mice lacking the ABC transporters A1 and G1. *Circ Res.* 2008;102:113−120. doi: 10.1161/CIRCRESAHA.107.161711

10. Rader DJ, Alexander ET, Weibel GL, Billheimer J, Rothblat GH. The role of reverse cholesterol transport in animals and humans and relationship to atherosclerosis. *J Lipid Res.* 2009;50(suppl):S189−S194. doi: 10.1194/jlr.R800088-JLR200

11. Chiesa G, Parolini C, Canavesi M, Colombo N, Sirtori CR, Fumagalli R, Franceschini G, Bernini F. Human apolipoproteins A-I and A-II in cell cholesterol efflux: studies with transgenic mice. *Arterioscler Thromb Vasc Biol.* 1998;18:1417−1423. doi: 10.1161/01.atv.18.9.1417

12. Bhatt A, Rohatgi A. HDL Cholesterol efflux capacity: cardiovascular risk factor and potential therapeutic target. *Curr Atheroscler Rep.* 2016;18:2. doi: 10.1007/s11883-015-0554-1

13. Sacks FM, Jensen MK. From high-density lipoprotein cholesterol to measurements of function: prospects for the development of tests for high-density lipoprotein functionality in cardiovascular disease. *Arterioscler Thromb Vasc Biol.* 2018;38:487−499. doi: 10.1161/ATVBAHA.117.307025

14. Murphy AJ, Westerterp M, Yvan-Charvet L, Tall AR. Anti-atherogenic mechanisms of high density lipoprotein: effects on myeloid cells. *Biochim Biophys Acta.* 2012;1821:513−521. doi: 10.1016/j.bbalip.2011.08.003

15. Lüscher TF, Landmesser U, von Eckardstein A, Fogelman AM. High-density lipoprotein: vascular protective effects, dysfunction, and potential as therapeutic target. *Circ Res.* 2014;114:171−182. doi: 10.1161/CIRCRESAHA. 114.300935

16. Pirillo A, Catapano AL, Norata GD. HDL in infectious diseases and sepsis. *Handb Exp Pharmacol.* 2015;224:483−508. doi: 10.1007/978-3-319-09665-0_15

17. Emini Veseli B, Perrotta P, De Meyer GRA, Roth L, Van der Donckt C, Martinet W, De Meyer GRY. Animal models of atherosclerosis. *Eur J Pharmacol.* 2017;816:3−13. doi: 10.1016/j.ejphar.2017.05.010

18. Jawien J. The role of an experimental model of atherosclerosis: apoE-knockout mice in developing new drugs against atherogenesis. *Curr Pharm Biotechnol.* 2012;13:2435−2439.

19. Lusis AJ. Atherosclerosis. *Nature.* 2000;407:233−241. doi: 10.1038/35025203

20. Getz GS, Reardon CA. Diet and murine atherosclerosis. *Arterioscler Thromb VascBiol.* 2006;26:242−249.doi:10.1161/01.ATV.0000201071.49029.17

21. Pászty C, Maeda N, Verstuyft J, Rubin EM. Apolipoprotein AI transgene corrects apolipoprotein E deficiency-induced atherosclerosis in mice. *J Clin Invest.* 1994;94:899−903. doi: 10.1172/JCI117412

22. Schaefer EJ, Santos RD, Asztalos BF. Marked HDL deficiency and premature coronary heart disease. *Curr Opin Lipidol.* 2010;21:289−297. doi: 10.1097/MOL.0b013e32833c1ef6

23. Williamson R, Lee D, Hagaman J, Maeda N. Marked reduction of high density lipoprotein cholesterol in mice genetically modified to lack apolipoprotein A-I. *Proc Natl Acad Sci U S A.* 1992;89:7134−7138. doi: 10.1073/pnas.89.15.7134

24. Marchesi M, Parolini C, Caligari S, Gilio D, Manzini S, Busnelli M, Cinquanta P, Camera M, Brambilla M, Sirtori CR, et al. Rosuvastatin does not affect human apolipoprotein A-I expression in genetically modified mice: a clue to the disputed effect of statins on HDL. *Br J Pharmacol.* 2011;164:1460−1468. doi: 10.1111/j.1476-5381.2011.01429.x

25. Arnaboldi F, Busnelli M, Cornaghi L, Manzini S, Parolini C, Dellera F, Ganzetti GS, Sirtori CR, Donetti E, Chiesa G. High-density lipoprotein deficiency in genetically modified mice deeply affects skin morphology: a structural and ultrastructural study. *Exp Cell Res.* 2015;338:105−112. doi: 10.1016/j.yexcr.2015.07.032

26. Parolini C, Bjorndal B, Busnelli M, Manzini S, Ganzetti GS, Dellera F, Ramsvik M, Bruheim I, Berge RK, Chiesa G. Effect of dietary components from antarctic krill on atherosclerosis in apoE-deficient mice. *Mol Nutr Food Res.* 2017;61:1700098. doi: 10.1002/mnfr.201700098.

27. Busnelli M, Manzini S, Hilvo M, Parolini C, Ganzetti GS, Dellera F, Ekroos K, Jänis M, Escalante-Alcalde D, Sirtori CR, et al. Liver-specific deletion of the Plpp3 gene alters plasma lipid composition and worsens atherosclerosis in apoE-/- mice. *Sci Rep.* 2017;7:44503. doi: 10.1038/srep44503

28. Parolini C, Vik R, Busnelli M, Bjørndal B, Holm S, Brattelid T, Manzini S, Ganzetti GS, Dellera F, Halvorsen B, et al. A salmon protein hydrolysate exerts lipid-independent anti-atherosclerotic activity in ApoE-deficient mice. *PLoS One.* 2014;9:e97598. doi: 10.1371/journal.pone.0097598

29. Busnelli M, Manzini S, Bonacina F, Soldati S, Barbieri SS, Amadio P, Sandrini L, Arnaboldi F, Donetti E, Laaksonen R, et al. Fenretinide treatment accelerates atherosclerosis development in apoE-deficient mice in spite of beneficial metabolic effects. *Br J Pharmacol.* 2020;177:328–345. doi: 10.1111/bph.14869

30. Daugherty A, Tall AR, Daemen MJAP, Falk E, Fisher EA, García-Cardeña G, Lusis AJ, Owens AP III, Rosenfeld ME, Virmani R; American Heart Association Council on Arteriosclerosis, Thrombosis and Vascular Biology; and Council on Basic Cardiovascular Sciences. Recommendation on design, execution, and reporting of animal atherosclerosis studies: a scientific statement from the American Heart Association. *Arterioscler Thromb Vasc Biol.* 2017;37:e131–e157. doi: 10.1161/ATV.0000000000000062

31. Parolini C, Caligari S, Gilio D, Manzini S, Busnelli M, Montagnani M, Locatelli M, Diani E, Giavarini F, Caruso D, et al. Reduced biliary sterol output with no change in total faecal excretion in mice expressing a human apolipoprotein A-I variant. *Liver Int.* 2012;32:1363–1371. doi: 10.1111/j.1478-3231.2012.02855.x

32. France DS, Hughes TE, Miserendino R, Spirito JA, Babiak J, Eskesen JB, Tapparelli C, Paterniti JR. Nonimmunochemical quantitation of mammalian apolipoprotein A-I in whole serum or plasma by nonreducing gel electrophoresis. *J Lipid Res.* 1989;30:1997–2004.

33. Manzini S, Busnelli M, Parolini C, Minoli L, Ossoli A, Brambilla E, Simonelli S, Lekka E, Persidis A, Scanziani E, et al. Topiramate protects apoE-deficient mice from kidney damage without affecting plasma lipids. *Pharmacol Res.* 2019;141:189–200. doi: 10.1016/j.phrs.2018.12.022

34. Manzini S, Pinna C, Busnelli M, Cinquanta P, Rigamonti E, Ganzetti GS, Dellera F, Sala A, Calabresi L, Franceschini G, et al. Beta2-adrenergic activity modulates vascular tone regulation in lecithin:cholesterol acyltransferase knockout mice. *Vascul Pharmacol.* 2015;74:114–121. doi: 10.1016/j.vph.2015.08.006

35. Livak KJ, Schmittgen TD. Analysis of relative gene expression data using real-time quantitative PCR and the 2(-Delta Delta C(T)) Method. *Methods.* 2001;25:402–408. doi: 10.1006/meth.2001.1262

36. Langmead B, Salzberg SL. Fast gapped-read alignment with Bowtie 2. *Nat Methods.* 2012;9:357–359. doi: 10.1038/nmeth.1923

37. Li B, Dewey CN. RSEM: accurate transcript quantification from RNA-Seq data with or without a reference genome. *BMC Bioinformatics.* 2011;12:323. doi: 10.1186/1471-2105-12-323

38. McCarthy DJ, Chen Y, Smyth GK. Differential expression analysis of multifactor RNA-Seq experiments with respect to biological variation. *Nucleic Acids Res.* 2012;40:4288–4297. doi: 10.1093/nar/gks042

39. R Core Team. R: A language and environment for statistical computing. 2017. https://www.r-project.org/.

40. Szklarczyk D, Morris JH, Cook H, Kuhn M, Wyder S, Simonovic M, Santos A, Doncheva NT, Roth A, Bork P, et al. The STRING database in 2017: quality-controlled protein-protein association networks, made broadly accessible. *Nucleic Acids Res.* 2017;45:D362–D368. doi: 10.1093/nar/gkw937

41. Edgar R, Domrachev M, Lash AE. Gene expression omnibus: NCBI gene expression and hybridization array data repository. *Nucleic Acids Res.* 2002;30:207–210. doi: 10.1093/nar/30.1.207

42. Zambelli F, Pesole G, Pavesi G. Pscan: finding over-represented transcription factor binding site motifs in sequences from co-regulated or co-expressed genes. *Nucleic Acids Res.* 2009;37(Web Server issue):W247–W252. doi: 10.1093/nar/gkp464

43. Sandelin A, Alkema W, Engström P, Wasserman WW, Lenhard B. JASPAR: an open-access database for eukaryotic transcription factor binding profiles. *Nucleic Acids Res.* 2004;32:D91–4. doi: 10.1093/nar/gkh012

44. Virtanen P, Gommers R, Oliphant TE, et al. SciPy 1.0--Fundamental algorithms for scientific computing in python. *arXiv.* Preprint posted online July 23, 2019. doi:arXiv:1907.10121.

45. Pedregosa F, Varoquaux G, Gramfort A, et al. Scikit-learn: machine learning in python. *J Mach Learn Res.* 2011;12:2825–2830.

46. Hunter JD. Matplotlib: a 2D graphics environment. *Comput Sci Eng.* 2007;9:90–95. doi: 10.1109/MCSE.2007.55

47. Waskom M, Botvinnik O, O'Kane D, et al. Seaborn. doi: 10.5281/zenodo.592845.

48. Harper M, Weinstein B, Simon C, Chebeei N, Swanson-Hysell TGB, Greco M, Zuidhof G. Python-ternary: ternary plots in python. 2015. doi: 10.5281/zenodo.34938

49. Rueden CT, Schindelin J, Hiner MC, DeZonia BE, Walter AE, Arena ET, Eliceiri KW. ImageJ2: ImageJ for the next generation of scientific image data. *BMC Bioinformatics.* 2017;18:529. doi: 10.1186/s12859-017-1934-z

50. Wickham H. Reshaping data with the reshape package. *J Stat Softw.* 2007;21:1–20.

51. Dinno A. Dunn's Test of Multiple Comparisons Using Rank Sums. 2017. https://cran.r-project.org/web/packages/dunn.test/dunn.test.pdf.

52. Kruskal WH, Wallis WA. Use of ranks in one-criterion variance analysis. *J Am Stat Assoc.* 1952;47:583. doi: 10.2307/2280779

53. Dunn OJ. Multiple comparisons using rank sums. *Technometrics.* 1964;6:241–252. doi: 10.1080/00401706.1964.10490181

54. Moos MP, John N, Gräbner R, Nossmann S, Günther B, Vollandt R, Funk CD, Kaiser B, Habenicht AJ. The lamina adventitia is the major site of immune cell accumulation in standard chow-fed apolipoprotein E-deficient mice. *Arterioscler Thromb Vasc Biol.* 2005;25:2386–2391. doi: 10.1161/01.ATV.0000187470.31662.fe

55. Gräbner R, Lötzer K, Döpping S, et al. Lymphotoxin beta receptor signaling promotes tertiary lymphoid organogenesis in the aorta adventitia of aged ApoE-/- mice. *J Exp Med.* 2009;206:233–248. doi: 10.1084/jem.20080752

56. Weih F, Gräbner R, Hu D, Beer M, Habenicht AJR. Control of dichotomic innate and adaptive immune responses by artery tertiary lymphoid organs in atherosclerosis. *Front Physiol.* 2012;3:226. doi:10.3389/fphys.2012.00226

57. Wang IM, Zhang B, Yang X, Zhu J, Stepaniants S, Zhang C, Meng Q, Peters M, He Y, Ni C, et al. Systems analysis of eleven rodent disease models reveals an inflammatome signature and key drivers. *Mol Syst Biol.* 2012;8:594. doi: 10.1038/msb.2012.24

58. Xi D, Zhao J, Zhao M, Fu W, Guo Z, Chen H. Identification of gene expression changes in the aorta of ApoE null mice fed a high-fat diet. *Genes (Basel).* 2017;8:289. doi: 10.3390/genes8100289

59. Raben N, Puertollano R. TFEB and TFE3: linking lysosomes to cellular adaptation to stress. *Annu Rev Cell Dev Biol.* 2016;32:255–278. doi: 10.1146/annurev-cellbio-111315-125407

60. Perera RM, Di Malta C, Ballabio A. MiT/TFE family of transcription factors, lysosomes, and cancer. *Annu Rev Cancer Biol.* 2019;3:203–222. doi: 10.1146/annurev-cancerbio-030518-055835

61. Plump AS, Scott CJ, Breslow JL. Human apolipoprotein A-I gene expression increases high density lipoprotein and suppresses atherosclerosis in the apolipoprotein E-deficient mouse. *Proc Natl Acad Sci U S A.* 1994;91:9607–9611. doi: 10.1073/pnas.91.20.9607

62. Yu EPK, Reinhold J, Yu H, Starks L, Uryga AK, Foote K, Finigan A, Figg N, Pung YF, Logan A, et al. Mitochondrial respiration is reduced in atherosclerosis, promoting necrotic core formation and reducing relative fibrous cap thickness. *Arterioscler Thromb Vasc Biol.* 2017;37:2322–2332. doi: 10.1161/ATVBAHA.117.310042

63. Eriksson O, Mohlin C, Nilsson B, Ekdahl KN. The human platelet as an innate immune cell: interactions between activated platelets and the complement system. *Front Immunol.* 2019;10:1590. doi: 10.3389/fimmu.2019.01590

64. Hansson GK, Hermansson A. The immune system in atherosclerosis. *Nat Immunol.* 2011;12:204–212. doi: 10.1038/ni.2001

65. Tabas I, Lichtman AH. Monocyte-macrophages and T cells in atherosclerosis. *Immunity.* 2017;47:621–634. doi: 10.1016/j.immuni.2017.09.008

66. Hu D, Mohanta SK, Yin C, Peng L, Ma Z, Srikakulapu P, Grassia G, MacRitchie N, Dever G, Gordon P, et al. Artery tertiary lymphoid organs control aorta immunity and protect against atherosclerosis via vascular smooth muscle cell lymphotoxin β receptors. *Immunity.* 2015;42:1100–1115. doi: 10.1016/j.immuni.2015.05.015

67. Yin C, Mohanta S, Ma Z, Weber C, Hu D, Weih F, Habenicht A. Generation of aorta transcript atlases of wild-type and apolipoprotein E-null mice by laser capture microdissection-based mRNA expression microarrays. *Methods Mol Biol.* 2015;1339:297–308. doi: 10.1007/978-1-4939-2929-0_20

68. Getz GS, Reardon CA. Apoprotein E as a lipid transport and signaling protein in the blood, liver, and artery wall. *J Lipid Res.* 2009;50(suppl):S156–S161. doi: 10.1194/jlr.R800058-JLR200

69. Angeli V, Llodrá J, Rong JX, Satoh K, Ishii S, Shimizu T, Fisher EA, Randolph GJ. Dyslipidemia associated with atherosclerotic disease systemically alters dendritic cell mobilization. *Immunity.* 2004;21:561–574. doi: 10.1016/j.immuni.2004.09.003

70. Sergin I, Evans TD, Razani B. Degradation and beyond: the macrophage lysosome as a nexus for nutrient sensing and processing in atherosclerosis. *Curr Opin Lipidol.* 2015;26:394–404. doi: 10.1097/MOL.0000000000000213

71. Settembre C, Ballabio A. Lysosome: regulator of lipid degradation pathways. *Trends Cell Biol.* 2014;24:743–750. doi: 10.1016/j.tcb.2014.06.006

72. Sergin I, Evans TD, Zhang X, Bhattacharya S, Stokes CJ, Song E, Ali S, Dehestani B, Holloway KB, Micevych PS, et al. Exploiting macrophage autophagy-lysosomal biogenesis as a therapy for atherosclerosis. *Nat Commun.* 2017;8:15750. doi: 10.1038/ncomms15750

73. Liao X, Sluimer JC, Wang Y, Subramanian M, Brown K, Pattison JS, Robbins J, Martinez J, Tabas I. Macrophage autophagy plays a protective role in advanced atherosclerosis. *Cell Metab.* 2012;15:545–553. doi: 10.1016/j.cmet.2012.01.022

74. Chinetti-Gbaguidi G, Daoudi M, Rosa M, Vinod M, Louvet L, Copin C, Fanchon M, Vanhoutte J, Derudas B, Belloy L, et al. Human alternative macrophages populate calcified areas of atherosclerotic lesions and display impaired RANKL-induced osteoclastic bone resorption activity. *Circ Res.* 2017;121:19–30. doi: 10.1161/CIRCRESAHA.116.310262

75. Hannun YA, Obeid LM. Sphingolipids and their metabolism in physiology and disease. *Nat Rev Mol Cell Biol.* 2018;19:175–191. doi: 10.1038/nrm.2017.107

76. Chatterjee SB, Dey S, Shi WY, Thomas K, Hutchins GM. Accumulation of glycosphingolipids in human atherosclerotic plaque and unaffected aorta tissues. *Glycobiology.* 1997;7:57–65. doi: 10.1093/glycob/7.1.57

77. Garner B, Priestman DA, Stocker R, Harvey DJ, Butters TD, Platt FM. Increased glycosphingolipid levels in serum and aortae of apolipoprotein E gene knockout mice. *J Lipid Res.* 2002;43:205–214.

78. Bismuth J, Lin P, Yao Q, Chen C. Ceramide: a common pathway for atherosclerosis? *Atherosclerosis.* 2008;196:497–504. doi: 10.1016/j.atherosclerosis.2007.09.018

79. Cheng JM, Suoniemi M, Kardys I, Vihervaara T, de Boer SP, Akkerhuis KM, Sysi-Aho M, Ekroos K, Garcia-Garcia HM, Oemrawsingh RM, et al. Plasma concentrations of molecular lipid species in relation to coronary plaque characteristics and cardiovascular outcome: results of the ATHERO-REMO-IVUS study. *Atherosclerosis.* 2015;243:560–566. doi: 10.1016/j.atherosclerosis.2015.10.022

80. Alayoubi AM, Wang JC, Au BC, Carpentier S, Garcia V, Dworski S, El-Ghamrasni S, Kirouac KN, Exertier MJ, Xiong ZJ, et al. Systemic ceramide accumulation leads to severe and varied pathological consequences. *EMBO Mol Med.* 2013;5:827–842. doi: 10.1002/emmm.201202301

81. Gong N, Wei H, Chowdhury SH, Chatterjee S. Lactosylceramide recruits PKCalpha/epsilon and phospholipase A2 to stimulate PECAM-1 expression in human monocytes and adhesion to endothelial cells. *Proc Natl Acad Sci U S A.* 2004;101:6490–6495. doi: 10.1073/pnas.0308684101

82. Li F, Zhang H. Lysosomal acid lipase in lipid metabolism and beyond. *Arterioscler Thromb Vasc Biol.* 2019;39:850–856. doi: 10.1161/ATVBAHA.119.312136

83. Zhang JR, Coleman T, Langmade SJ, Scherrer DE, Lane L, Lanier MH, Feng C, Sands MS, Schaffer JE, Semenkovich CF, et al. Niemann-Pick C1 protects against atherosclerosis in mice via regulation of macrophage intracellular cholesterol trafficking. *J Clin Invest.* 2008;118:2281–2290. doi: 10.1172/JCI32561

84. Sekiya M, Osuga J, Nagashima S, Ohshiro T, Igarashi M, Okazaki H, Takahashi M, Tazoe F, Wada T, Ohta K, et al. Ablation of neutral cholesterol ester hydrolase 1 accelerates atherosclerosis. *Cell Metab.* 2009;10:219–228. doi: 10.1016/j.cmet.2009.08.004

85. Aiello RJ, Brees D, Bourassa PA, Royer L, Lindsey S, Coskran T, Haghpassand M, Francone OL. Increased atherosclerosis in hyperlipidemic mice with inactivation of ABCA1 in macrophages. *Arterioscler Thromb Vasc Biol.* 2002;22:630–637. doi: 10.1161/01.atv.0000014804.35824.da

BASIC SCIENCES - AL